

# Compositional Clustering for Multi-Label Few-Shot Learning

Zeqian Li<sup>a</sup>, Xinlu He<sup>a</sup>, Jacob Whitehill<sup>a,\*</sup>

<sup>a</sup>Worcester Polytechnic Institute, 100 Institute Road, 01609, Worcester, USA

---

## Abstract

We consider a new kind of clustering problem in which clusters need not be independent of each other, but rather can have compositional relationships with other clusters (e.g., a dataset contains images of rectangles, images of circles, and images of both). This task is motivated by recent work on compositional few-shot learning and embedding models [1, 17] that are optimized to distinguish the label *sets*, not just the individual labels, assigned to the examples. To tackle this clustering problem, we propose three new algorithms: Compositional Affinity Propagation (CAP), Compositional  $k$ -means (CKM), and Greedy Compositional Reassignment (GCR). These new methods can both partition examples into coherent groups and infer the compositional structure among the groups automatically. We show promising results, compared to popular algorithms such as Gaussian mixtures, Fuzzy  $c$ -means, and Agglomerative Clustering, on the OmniGlot and LibriSpeech datasets that are widely used in few-shot learning research. Our work has applications to open-world multi-object image recognition and speaker diarization with simultaneous speech from multiple speakers.

*Keywords:* Few-Shot Learning, Compositional Learning, Clustering Algorithms, Embedding Models, Speaker Diarization, Affinity Propagation

---

## 1. Introduction

We consider a new kind of clustering problem in which clusters have compositional structure, in the sense that each example in one cluster may exhibit the *union* of the

---

\*Corresponding author

Email addresses: [zli14@wpi.edu](mailto:zli14@wpi.edu) (Zeqian Li), [xhe4@wpi.edu](mailto:xhe4@wpi.edu) (Xinlu He), [jrwhitehill@wpi.edu](mailto:jrwhitehill@wpi.edu) (Jacob Whitehill)

properties found in another set of clusters. The goal is not just to partition the data into distinct and coherent groups, but also to infer the compositional relationships among the groups. This scenario arises in speaker diarization (i.e., infer who is speaking when from an audio wave) in the presence of simultaneous speech from multiple speakers [6, 31], which occurs frequently in real-world speech settings: The audio at each time  $t$  is generated as a *composition* of the voices of all the people speaking at time  $t$ , and the goal is to cluster the audio samples, over all timesteps, into sets of speakers. Hence, if there are 2 people who sometimes speak by themselves and sometimes speak simultaneously, then the clusters would correspond to the speaker sets  $\{1\}$ ,  $\{2\}$ , and  $\{1, 2\}$  – the third cluster is not a third independent speaker, but rather the composition of the first two speakers. An analogous scenario arises in open-world (i.e., test classes are disjoint from training classes) multi-label object recognition when clustering images such that each image may contain multiple objects from a fixed set (e.g., the shapes in Figure 1). In some scenarios, the *composition* function that specifies how examples are generated from other examples might be as simple as superposition by element-wise maximum or addition. However, a more powerful form of composition – and the main motivation for our work – is enabled by *compositional embedding models*, which are a new technique for few-shot learning.

**Compositional embedding models:** Standard (non-compositional) embedding models for few-shot learning such as FaceNet [25] and x-vector [26] have an embedding function  $f^{\text{emb}}$  (typically a neural network) that maps each example (e.g., image, audio clip) into an embedding space so that examples with the same label are mapped close together, and examples with different labels are mapped far apart. Compositional embeddings [1, 17] go a step further and are trained to separate not just individual labels, but entire *sets* of labels. As an example of how this is performed using the approach by [17], suppose an image collection contains some images of rectangles, some of circles, and some of both (see Figure 1). Then the embedding function  $f^{\text{emb}}$  would induce three clusters in the embedding space corresponding to  $\{\text{rectangle}\}$ ,  $\{\text{circle}\}$  and  $\{\text{rectangle, circle}\}$ . In addition to  $f^{\text{emb}}$ , compositional embedding models have a *composition* function  $g$  that takes the embedding vectors  $x_a, x_b$  of two examples and computes a set relationship between them. For instance,  $g(x_a, x_b)$  might return another vector in the same embedding space corresponding to where an example containing the *union* of the labels in the two

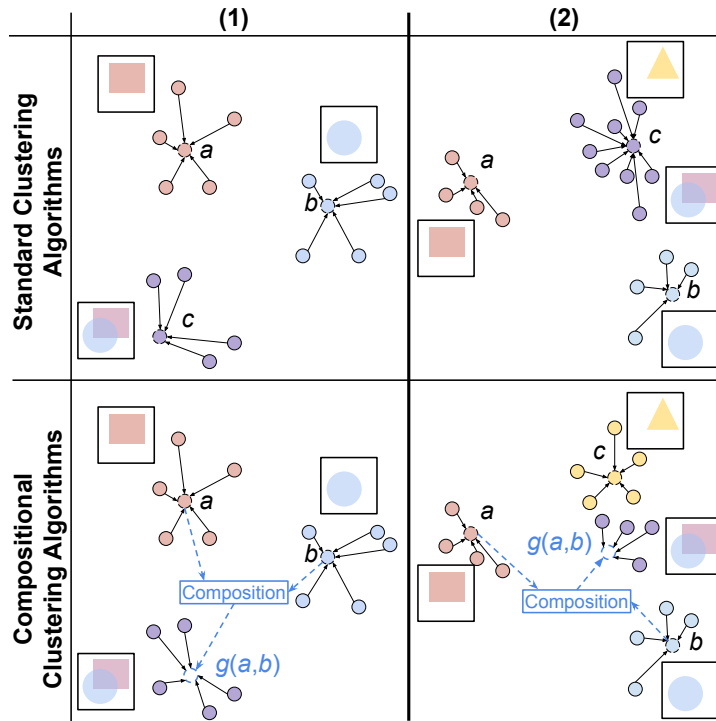


Figure 1: *Conceptual overview of our paper*: Scenario (1) shows clusters of images (containing rectangles, circles, or both) and their assigned exemplars (for exemplar-based methods) or centroids (for centroid-based methods)  $a, b, c$ , etc. Each arrow represents the assignment of an example to its cluster exemplar/centroid. Standard clustering algorithms such as  $k$ -means or Affinity Propagation detect 3 clusters that are independent of each other. Compositional clustering algorithms like CAP, CKM, and GCR can infer that each example in the bottom/purple cluster is *composed* (via  $g$ ) of examples from clusters  $a$  &  $b$ . Scenario (2) illustrates how modeling compositionality can enable CAP and CKM to find purer clusters by not lumping the two sets of images (some with triangles, and some with rectangles & circles) together.

inputs would lie – see Figure 1 (lower left). In particular, the training objective is for  $g(x_a, x_b) \approx x_{ab}$ , where  $x_{ab}$  is the embedding of an example containing *both* classes  $a$  and  $b$ . At test time,  $f^{\text{emb}}$  and  $g$  are used together (along with a support set of few-shot examples) to infer the *set* of labels in an example. A similar idea of training the embedding network so that set operations such as union, difference, and containment can be computed on the embedding space [27, 32], or of using the embedding space to synthesize feature vectors with specific properties [11], has been pursued in several other recent works as well.

**Compositional clustering methods:** In this paper we present and evaluate three novel algorithms for tackling the “compositional clustering” problem: (1) **Compositional  $k$ -means (CKM)**, which is a centroid-based clustering method; (2) **Compositional Affinity Propagation (CAP)**, which is an exemplar-based method; and (3) **Greedy Compositional Reassignment (GCR)**, which can be used in tandem with any standard clustering algorithm. All three of these methods have the ability to assign each example to either a “singleton” cluster corresponding to a single class (e.g., a single speaker, or a single object) *or* to a “compositional” cluster corresponding to the union of multiple classes (e.g., a set of speakers, or a set of objects). CKM and CAP have the additional ability to harness the compositional structure of the data to partition them more accurately than is possible with standard clustering algorithms.

As a conceptual illustration, see Figure 1. In scenario (1) (left half of the figure), there are three sets of images – some contain circles, some contain rectangles, and some contain both. Standard clustering algorithms such as Affinity Propagation and  $k$ -means can separate the data correctly into three clusters. However, a compositional clustering algorithm such as CKM, CAP, or GCR can also infer that the cluster shown in purple in the bottom-left is actually a *compositional cluster* in which each example contains *both* objects from the first two clusters. Scenario (2) in the figure shows how modeling the compositionality can yield a more accurate partition: whereas standard clustering algorithms will lump together the images containing triangles with those containing a composition of rectangles and circles, CAP and CKM can identify this relationship automatically and thereby obtain purer clusters.

**General Workflow:** Here is how a compositional clustering algorithm can be used in practice. Suppose that the set of classes at test time are different from those during

training (e.g., open-world object recognition, or speaker diarization). The first step is to (1) train a compositional embedding model (e.g., using the methodology in [1] or [17]) with both an embedding function  $f^{\text{emb}}$  (e.g., with triplet loss, ArcFace loss [8], etc.) as well as a composition function  $g$  that computes the location in the embedding space corresponding to the *set union* of the classes represented in its two input embeddings. (This only needs to be done once and can then be reused.) Next, (2) compute the embeddings of all the speaker utterances (or images) in the dataset; we denote the set of these embeddings as  $\mathcal{X} = \{x_1, \dots, x_n\}$ . (3) Pass  $\mathcal{X}$ , as well as the composition network  $g$ , as input to the compositional clustering algorithm (CAP, CKM, or GCR). The clustering algorithm then (4) infers the cluster label – which could be either a *singleton* (a single speaker in isolation, or a single object appearing by itself) or a *set* (multiple speakers in simultaneous speech, or multiple objects co-occurring in an image) – of each example.

**Contributions:** (1) We consider the computational problem of clustering data with compositional structure, particularly as afforded by compositional embedding models, in the setting where (a) the test classes are disjoint from training classes, (b) each example can belong to multiple classes, and (c) no information about the test classes (neither a support set, nor a semantic description) is given. To our knowledge, this particular task has not been tackled previously. We also define a new accuracy metric, the Compositional Rand Index, for this problem. (2) We present three novel clustering algorithms – CAP, CKM, and GCR – that can partition data and infer their compositional structure automatically. (3) We illustrate how these new methods can infer the clusters, as well as their compositional relationships, more accurately compared to standard clustering algorithms (Affinity Propagation,  $k$ -means, Gaussian mixtures, etc.) in two challenging application areas: speaker recognition from speech with multiple overlapping speakers, and multi-label object recognition in open-world scenarios.

## 2. Related Work

### 2.1. Multi-Label Few-Shot and Zero-Shot Learning

The past 5 years have seen significant growth in the fields of multi-label few-shot and zero-shot learning (e.g., [16, 21, 7, 14]). Much of this work relies on the existence of a knowledge graph such as WordNet [20], a word embedding space such as GloVe

[23], or external attribute vectors, to represent relationships among classes and thereby enable the model to generalize to data from unseen classes at test time. In contrast, the compositional embedding models of [1] and [17], and thus our work as well, make no such assumption – each class can be completely independent of each other. To our best knowledge, no prior work has investigated how to *cluster* examples automatically when the test classes are disjoint from training classes, when no support sets are provided, and when no semantic information about the test classes is provided. (Note that, when a support set of few-shot examples is provided for the test classes, then the “clustering” problem becomes trivial – the examples can be grouped based just on their estimated label vectors.)

## 2.2. Clustering

To our best knowledge, no currently used clustering algorithm exists that can both cluster a dataset and infer the compositionality among clusters. Below we describe the most similar techniques within the clustering literature and describe how they differ from our work.

**Mixture models**, such as the Mixture of Gaussians fit using Expectation-Maximization, the Dirichlet mixture process [5], and the fuzzy  $k$ -means clustering algorithm [3], extend the standard  $k$ -means algorithm by “softly” assigning each data point to a probability distribution over the mixture components instead of giving a “hard” assignment like in  $k$ -means. Importantly, these approaches assume that each data point is generated by a *single* cluster, and the probability distribution expresses the uncertainty over which cluster it is. They can capture compositionality only in a limited sense by assuming that examples that lie between two (or more) cluster centroids belong to both (or all) of these clusters. These methods cannot distinguish between an example that is unconfidently assigned to a single cluster (thus resulting in high entropy over the mixture components for that example), from an example that is confidently assigned to multiple clusters. Moreover, they will fail if the compositional cluster (e.g., the purple cluster in the left half of Figure 1) does not lie near the mean of its constituent singleton clusters (the red and blue clusters in the figure).

**Hierarchical clustering algorithms** create a tree (dendrogram) such that the  $n$  leaf nodes correspond 1-to-1 to the examples in the dataset, and each internal node  $i$

represents a cluster whose members consist of all the leaf nodes descending from  $i$ . Internal nodes closer to the root correspond to higher-level abstractions of the data. Hierarchical clustering algorithms can work either top-down by splitting clusters or bottom-up by merging clusters, until some clustering criterion is reached. One popular variant is *Agglomerative Clustering* using the Ward Jr [28] criterion, which seeks to minimize the variance within each cluster. In all cases, hierarchical clustering algorithms assign each example to a sequence of clusters of increasing generality, starting from the internal node just above the leaf all the way up to the root node, such that each parent cluster captures the *intersection* of the characteristics of the child clusters. In contrast, our proposed method can assign each example to contain the *union* of the properties in multiple clusters; this is tantamount to a dendrogram where each example is connected by an edge to multiple parent nodes, thus yielding a directed acyclic graph rather than a tree.

**Multi-view clustering algorithms** (e.g., Bickel and Scheffer [4]) partition the feature space into multiple subsets, each corresponding to a different “view” of the data. For instance, each example might be a video and thus have both auditory and visual features associated with it. The structure of the data from one view can provide implicit supervision when clustering using the other views. These methods do not have any inherent ability to model compositionality. Franklin and Frank [9] recently proposed a method for “compositional clustering in task structure learning”, but their method is more akin to multi-view clustering, and the compositionality pertains to how they tackled a control problem (separately addressing the reward and transition functions), not the clustering problem itself.

**Exemplar-based** clustering algorithms differ from **centroid-based** algorithms in how clusters are represented: In the former, each cluster is represented by a specific example in the dataset; in contrast, the latter (e.g.,  $k$ -means) may compute a function of the examples (e.g., the mean) to represent the cluster. One of the mostly widely used exemplar-based clustering algorithms is Affinity Propagation [10].

### 3. Approach I: Compositional Affinity Propagation (CAP)

The first compositional clustering method we propose is called Compositional Affinity Propagation, which is an exemplar-based clustering method that is commonly used for

speaker diarization to group clusters of utterances into distinct speakers [30, 18]. CAP is based on an undirected probabilistic graphical model whose likelihood is approximately optimized using discrete optimization. Before describing CAP in detail, we first review the standard Affinity Propagation method [10] below.

### 3.1. Review of Affinity Propagation

Let  $\mathcal{X} = \{x_1, \dots, x_n\} \subset \mathbb{R}^p$  be a dataset, and let  $\mathcal{C} = \{1, \dots, n\} \doteq [n]$  be the set of indices of the (embedded) examples in  $\mathcal{X}$ . Next, let  $c_1, \dots, c_n \in \mathcal{C}$  be the cluster assignments: Each  $c_i$  denotes the *exemplar* representing the cluster to which example  $i$  belongs; if example  $i$  itself is the exemplar for some other example  $j \neq i$ , then we require  $c_i = i$ . For instance, if  $\mathcal{X}$  contains  $n = 3$  examples, the first two of which belong to the same cluster and the third of which belongs to its own cluster, then we might have  $c_1 = 2, c_2 = 2, c_3 = 3$  (or possibly  $c_1 = 1, c_2 = 1, c_3 = 3$ ). Let  $S : \mathcal{C} \times \mathcal{C} \rightarrow [-\infty, 0]$  map from a pair of example indices to the negative (squared) distance between the examples, i.e.,  $S(i, j) = -\|x_i - x_j\|^2$  for  $i \neq j$ ; and let  $S$  map to a constant value for  $i = j$ , i.e.,  $S(i, i) = \gamma$ , where  $\gamma$  is the “preference” (a hyperparameter) that  $x_i$  is an exemplar, where larger negative values discourage those examples from becoming exemplars. From these definitions, we can formulate the following constrained optimization problem:

$$\arg \max_{c_1, \dots, c_n \in \mathcal{C}} \sum_{i=1}^n S(i, c_i) \quad \text{s.t.} \quad (\exists i : c_i = k) \implies c_k = k$$

The objective is the sum of distances between each point and its assigned exemplar, and the constraints enforce consistency that examples used by others as exemplars also designate themselves as exemplars. The optimization process has to weigh the cost  $\gamma$  of creating a new cluster against assigning examples to existing exemplars that are farther away.

**Illustration:** Given an appropriate choice for the  $\gamma$ , Affinity Propagation would yield the results shown in the top half of Figure 1. In particular, in scenario (1), the cluster shown in purple would be identified as an independent cluster with exemplar  $c$ , and in scenario (2), the cluster shown in purple would contain the images with triangles as well as those composed of rectangles and circles.

**Inference:** Frey and Dueck [10] showed a procedure to find approximately optimal solutions by defining a *factor graph* to represent the variables and constraints, where  $S$

is interpreted as containing log-likelihoods, and then applying loopy belief propagation. This results in a new optimization problem where the goal is to find maximum a posteriori (MAP) solutions to  $\arg \max_{c_1, \dots, c_n \in \mathcal{C}} P(c_1, \dots, c_n \mid S)$ . where probability distribution  $P$  is understood to encode the constraints. Specifically, the factor graph contains variable nodes to represent  $c_1, \dots, c_n$  and factor nodes to represent both the log-likelihoods  $S(1, \cdot), \dots, S(n, \cdot)$  and a set of *constraints*  $\delta_1, \dots, \delta_n$ . Each  $\delta_k$  encodes whether  $c_k$  is compatible with the other  $c_{k' \neq k}$ :

$$\delta_k(c_1, \dots, c_n) = \begin{cases} -\infty & \text{if } \exists i : (c_i = k) \wedge (c_k \neq k) \\ 0 & \text{otherwise} \end{cases} \quad (1)$$

Given the factor graph, a sequence of “messages” (functions  $\alpha, \rho : [n] \times [n] \times \mathcal{C} \rightarrow [-\infty, 0]$ ) is passed back and forth between the variable and factor nodes. Each variable  $i$  sends a message  $\rho_{i \rightarrow k}(c_i)$  to constraint  $k$ , and each constraint  $k$  sends a message  $\alpha_{i \leftarrow k}(c_i)$  to variable  $i$ , about the likelihood of each possible value of  $c_i$ . The values of  $\alpha$  and  $\rho$  are determined by the max-product algorithm for loopy belief propagation [29] applied to the factor graph (see the Appendices). To find an approximate MAP estimate for all the  $c_i$ , we alternate between computing the  $\alpha$ ’s and the  $\rho$ ’s. Finally, after any number of iterations, we compute:

$$c_i^{\text{MAP}} = \arg \max_{c_i} \left[ \sum_k \alpha_{i \leftarrow k}(c_i) + S(i, c_i) \right]$$

Frey and Dueck [10] also presented an efficient ( $O(n^2)$ ) method to calculate all the messages for each iteration.

### 3.2. Procedure: Compositional Affinity Propagation

Here we describe our proposed Compositional Affinity Propagation algorithm. At a high level, CAP innovates on classic AP by allowing each cluster to be represented by not just a single example (“singleton” cluster), but rather an entire *set* of examples (“compositional” cluster). Importantly, the examples in this set need not be semantically similar or lie close to each other in the feature space; rather, the *union* of the characteristics of the examples in this set should be present in *each* of the examples belonging to the compositional cluster. In terms of the inference procedure, CAP is somewhat more

complex than standard AP due to the need, as part of the max-product algorithm, to compute the maximum values of many subsets efficiently (FindAllMaxes).

Let  $\mathcal{X} = \{x_1, \dots, x_n\} \subset \mathbb{R}^p$  be a dataset. Let  $\mathcal{C} \subset 2^{[n]} \setminus \emptyset$  be the set of compositions of examples in  $\mathcal{X}$  under consideration, where we assume  $\mathcal{C}$  contains all the singletons, i.e.,  $\{i\} \in \mathcal{C}, i = 1, \dots, n$ . Let  $d = \max_{c \in \mathcal{C}} |c|$ , i.e., the size of the largest composition under consideration. To identify which compositions contain (or do not contain) each example  $k$ , define functions  $\phi, \bar{\phi} : [n] \rightarrow \mathcal{C}$  such that  $\phi(k) = \{c \in \mathcal{C} : c \ni k\}$  and  $\bar{\phi}(k) = \mathcal{C} \setminus \phi(k)$ .

Let  $f$  be defined as in standard Affinity Propagation. We further assume there is a function  $g : 2^{\mathcal{X}} \setminus \emptyset \rightarrow \mathbb{R}^p$  that consumes a set of examples and produces another vector representing their composition; for singleton sets, we let  $g$  be the identity function, i.e.,  $g(\{x\}) = x$ . For instance,  $g$  could be the element-wise maximum to perform pixel-wise superposition of the images; for word embeddings, it could be element-wise addition [2]; or it could be a trained neural network within a compositional embedding model. We define  $S : [n] \times \mathcal{C} \rightarrow [-\infty, 0]$  to measure the distance between each example and each composition:  $S(i, c) = -\|x_i - g(\{x_k : k \in c\})\|$  for  $c \neq \{i\}$ , and  $S(i, \{i\}) = \gamma$  is a hyperparameter for each example.

Finally, define  $c_1, \dots, c_n \in \mathcal{C}$  as the assignment of which example belongs to which cluster. If  $c_i = \{k\}$  (i.e., a singleton), then example  $i$  belongs to a *singleton* cluster with exemplar  $x_k$ . If  $|c_i| \geq 2$ , then example  $i$  belongs to the cluster with a *compositional exemplar*  $g(\{x_k : k \in c_i\})$ , i.e., the composition of all the examples in  $c_i$ . Note that, in general, compositional exemplars are not members of  $\mathcal{X}$ . In CAP, we require that, whenever some example  $i$  designates its exemplar either to *be* example  $k$  ( $c_i = \{k\}$ ), or to *include* example  $k$  ( $c_i \ni k$ ), then example  $k$  must designate itself as an exemplar ( $c_k = \{k\}$ ). Example: if  $\mathcal{X} = \{x_1, x_2, x_3, x_4\}$  and we allow compositions of size at most 2, then  $\mathcal{C} = \{\{1\}, \{2\}, \{3\}, \{4\}, \{1, 2\}, \{1, 3\}, \{1, 4\}, \{2, 3\}, \{2, 4\}, \{3, 4\}\}$ ; if  $x_1$  and  $x_2$  each constitutes its own cluster and the last two examples are both assigned to the composition of the first two clusters, then we would have  $c_1 = \{1\}, c_2 = \{2\}, c_3 = c_4 = \{1, 2\}$ .

Our new constrained optimization problem is thus:

$$\arg \max_{c_1, \dots, c_n \in \mathcal{C}} \sum_{i=1}^n S(i, c_i) \quad \text{s.t.} \quad (\exists i : c_i \ni k) \implies c_k = \{k\}$$

Importantly, the optimization objective incurs *no additional cost* when an example is

assigned to a compositional exemplar  $c_k$  as long as all of the examples  $k' \in c_k$  have themselves already been designated as exemplars.

**Illustration:** Given an appropriate choice for  $\gamma$ , CAP would yield the results shown in the bottom half of Figure 1. In scenario (1), the cluster shown in purple would be identified as a cluster with a *compositional exemplar*. In scenario (2), the compositional structure identified by the algorithm could help it to separate the images containing triangles from those containing both a rectangle and a circle.

### 3.2.1. Inference

As with standard Affinity Propagation, we find a MAP estimate for each  $c_i$  by defining a factor graph and computing and passing messages between the variables and the factors. We adjust the definition of  $\delta_k$  to be:

$$\delta_k(c_1, \dots, c_n) = \begin{cases} -\infty & \text{if } \exists i : (c_i \ni k) \wedge (c_k \neq \{k\}) \\ 0 & \text{otherwise} \end{cases} \quad (2)$$

In the Appendices, we derive a procedure to compute all the messages  $\alpha, \rho$  efficiently; see Algorithm 1. (Python code is also available). At a high level, the derivation of CAP is similar to that of standard Affinity Propagation and follows the max-product algorithm. At a low level, most of the derivation involves algebraic simplifications to reduce the amount of computation, and also in devising an efficient approach find the maxima of many subsets efficiently.

**Theorem 3.1.** *Let  $n$  be the number of examples in a dataset  $\mathcal{X}$ , and let  $d$  be the largest element in the set  $\mathcal{C}$  containing all compositions under consideration. Then Algorithm 1 implements message passing (i.e., computation of sufficient statistics of  $\alpha$  and  $\rho$ ) for Compositional Affinity Propagation and operates in time  $O(dn^{d+1})$  per iteration.*

*Proof.* See Appendices. □

### 3.3. $CAP_{\subset}$ : An Approximation to CAP

To improve the scalability of CAP, we can apply it to a randomly selected subset of examples  $\tilde{\mathcal{X}} \subset \mathcal{X}$  and infer the cluster assignments  $\tilde{c}_1, \dots, \tilde{c}_{|\tilde{\mathcal{X}}|}$ . Let  $\mathcal{E} = \{\tilde{c}_i\}_{i=1}^{|\tilde{\mathcal{X}}|} \subset \mathcal{C}$  be the set of *unique* exemplars (singleton or compositional) inferred for  $\tilde{\mathcal{X}}$ . Then, for each example  $x_i$  in the original dataset  $\mathcal{X}$ , we designate its exemplar to be the  $\tilde{c}_i \in \mathcal{E}$  that is closest to it  $x_i$  according to  $f$ . Specifically, we assign  $c_i = \arg \min_{\tilde{c}_i \in \mathcal{E}} \|x_i, g(\{x_j : j \in \tilde{c}_i\})\|$ .

We call this method  $CAP_{\subset}$ .

---

**Algorithm 1** Compositional Affinity Propagation (CAP)

---

**CAP**( $S, \mathcal{C}$ ):

$$\begin{aligned} \phi(k) &\leftarrow \{c \in \mathcal{C} : c \ni k\}, \quad \bar{\phi}(k) \leftarrow \mathcal{C} \setminus \phi(k) \quad \forall k \\ q(i, c_i) &\leftarrow 0 \quad \forall i, c_i \\ a(i, k) &\leftarrow 0, \quad \bar{a}(i, k) \leftarrow 0 \quad \forall i, k \\ \text{while not converged do} \\ &\quad b, \bar{b}, h \leftarrow \text{ComputeRhoStats}(S, \mathcal{C}, \phi, \bar{\phi}, a, \bar{a}, q) \\ &\quad a, \bar{a}, q \leftarrow \text{ComputeAlphaStats}(\mathcal{C}, b, \bar{b}, h) \\ \text{end while} \\ \text{return } &\arg \max_{c_i} (q(i, c_i) + S(i, c_i)) \quad \forall i \end{aligned}$$
**ComputeRhoStats**( $S, \mathcal{C}, \phi, \bar{\phi}, a, \bar{a}, q$ ):

$$\begin{aligned} \text{for } i = 1, \dots, n \text{ do} \\ &\quad r, s \leftarrow \text{FindAllMaxes}(S(i, \cdot) + q(i, \cdot), \mathcal{C}, \phi, \bar{\phi}) \\ \text{for } k = 1, \dots, n \text{ do} \\ &\quad b(i, k) \leftarrow \max(r(k) - a(i, k), s(k) - \bar{a}(i, k)) \\ &\quad \bar{b}(i, k) \leftarrow s(k) - \bar{a}(i, k) \\ \text{end for} \\ \text{end for} \\ \text{for } k = 1, \dots, n \text{ do} \\ &\quad h(k) \leftarrow S(k, \{k\}) + q_k(\{k\}) - a(k, k) \\ \text{end for} \\ \text{return } &b, \bar{b}, h \end{aligned}$$
**ComputeAlphaStats**( $\mathcal{C}, b, \bar{b}, h$ ):

$$\begin{aligned} \text{for } k = 1, \dots, n \text{ do} \\ \text{for } i = 1, \dots, n \text{ do} \\ \text{for } k = 1, \dots, n \text{ do} \\ \text{if } i = k \text{ then} \\ &\quad a(i, k) \leftarrow e(k) \\ &\quad \bar{a}(i, k) \leftarrow \bar{e}(k) \\ \text{else} \\ &\quad a(i, k) \leftarrow h(k) + e(k) - b(i, k) \\ &\quad \bar{a}(i, k) \leftarrow \max(\bar{b}(k, k) + \bar{e}(k) - \bar{b}(i, k), h(k) + e(k) - b(i, k)) \\ \text{end if} \\ \text{end for} \\ \text{end for} \\ \text{end for} \\ \text{for } i = 1, \dots, n \text{ do} \\ &\quad q^*(i) \leftarrow \sum_{k'} \bar{a}(i, k') \\ \text{for } c_i \in \mathcal{C} \text{ do} \\ &\quad q(i, c_i) \leftarrow q^*(i) + \sum_{k' \in c_i} (a(i, k') - \bar{a}(i, k')) \\ \text{end for} \\ \text{end for} \\ \text{return } &a, \bar{a}, q \end{aligned}$$


---

---

**Algorithm 2** Finding Maxima of Many Subsets

---

```

FindAllMaxes( $q, \mathcal{C}, \phi, \bar{\phi}$ ):
   $r(k) \leftarrow \max q(\phi(k)) \quad \forall k$ 
   $s(k) \leftarrow -\infty \quad \forall k$ 
  for  $j = 1, \dots, d$  do
    for  $\tau = \{t_1, \dots, t_{j-1}\}$  s.t.  $\exists t_j > t_{j-1} : \{t_1, \dots, t_j\} \in \mathcal{C}$  do
       $\psi_\tau \leftarrow \{\{t_1, \dots, t_{j-1}, t_j\}\}_{t_j > t_{j-1}} \cap \mathcal{C}$ 
       $c^1, c^2 \leftarrow \arg \max_{c \in \psi_\tau}^{1,2} q(c)$ 
      for  $k = 1, \dots, n$  do
        if  $c^1 \in \phi(k)$  then
           $s(k) \leftarrow \max(s(k), q(c^1))$ 
        else if  $c^2 \in \bar{\phi}(k)$  then
           $s(k) \leftarrow \max(s(k), q(c^2))$ 
        end if
      end for
    end for
  end for
  return  $r, s$ 

```

---

#### 4. Approach II: Compositional $k$ -means

The second compositional clustering algorithm we propose is called Compositional  $k$ -means (CKM). In contrast to CAP, which uses discrete optimization to assign examples to exemplars, CKM uses gradient descent to minimize a sum of squared distances by adjusting the real-valued cluster centroids. Like CAP, the CKM method can potentially cluster the data in Figure 1 more accurately by harnessing the composition function  $g$  to infer which examples belong to singleton clusters versus compositional clusters. CKM is a centroid-based method rather than an exemplar-based clustering method. Hence, each cluster assignment variable  $c_i$  is a subset of  $[k]$  (rather than of  $[n]$ , like with CAP).

##### 4.1. Review of classic $k$ -means

Given the number of clusters  $k$  as input, classic  $k$ -means seeks to assign each of the  $n$  examples to one of the  $k$  clusters (denoted  $c_i \in [k]$  for each  $i$ ), so as to minimize the following sum of squared distances (SSD):

$$\text{SSD}(\{m_j\}_{j=1}^k, \{c_i\}_{i=1}^n) = \sum_{i=1}^n \|x_i - m_{c_i}\|^2 \quad (3)$$

Here, each  $m_j \in \mathbb{R}^p$  is a cluster centroid, and each  $c_i \in [k]$  is a cluster index. To (locally) minimize the SSD, two steps are executed in alternation until convergence:

1. Assign each  $x_i$  to the cluster  $j$  whose centroid  $m_j \in \mathbb{R}^p$  is closest to  $x_i$ ; and
2. Compute each centroid  $m_j$  as the mean of the points assigned to cluster  $j$ .

In particular, the second step is the closed-form minimizer of Equation 3 w.r.t. the centroids  $m_j$ .

**Convergence:** Since each of these steps is guaranteed not to increase the SSD, and since a lower bound on SSD is always 0, the algorithm is guaranteed to converge to a local minimum.

#### 4.2. Procedure: Compositional $k$ -means

Let the number of singleton clusters  $k$  (e.g., the number of individual speakers in the audio, or the number of basic object classes in the image set) be known, and let  $\mathcal{K} \subset 2^{[k]}$  be a set of possible compositions of the singleton clusters, where we require that  $\mathcal{K}$  contains all the singletons, i.e.,  $\{i\} \in \mathcal{K}, i = 1, \dots, k$ . Assume composition function  $g$  is differentiable. CKM seeks to assign each  $x_i$  to *either* one of  $k$  singleton clusters (a single person speaking in isolation, or a single object by itself) *or* to a compositional cluster (the composition of multiple speakers in an audio, or multiple objects in an image) so as to minimize the following sum of squared distances:

$$\text{SSD}(\{m_{\{j\}}\}_{j=1}^k, \{c_i\}_{i=1}^n) = \sum_{i=1}^n \|x_i - m_{c_i}\|^2 \quad (4)$$

where each compositional centroid  $m_\eta = g(\{m_{\{j\}}\}_{j \in \eta})$  (for  $\eta \in \mathcal{K}$  and  $|\eta| > 1$ ) is computed using the composition function  $g$ . (Note the small difference in notation compared to Equation 3 in the subscript of  $m$  so as to emphasize that a cluster centroid may represent the composition of other clusters.)

Like the classic  $k$ -means, the SSD is a function of the *singleton* cluster centroids (i.e.,  $m_{\{1\}}, \dots, m_{\{k\}}$ ). Unlike classic  $k$ -means, the CKM method can assign each example to either a singleton or a compositional cluster. By adjusting the singleton centroids, the locations of the *compositional* centroids – and thus the SSD value itself – are also affected due to their dependence via  $g$ .

At a high level, CKM works as follows: After initializing the singleton cluster centroids randomly and computing the compositional centroids using  $g$ , a two-step alternating procedure is executed whereby (a) each example  $x_i$  is assigned to the closest centroid

(either singleton or compositional), and (b) the *singleton* centroids  $m_{\{1\}}, \dots, m_{\{k\}}$  are adjusted using gradient descent (with learning rate  $\epsilon$ ) to reduce the SSD in Equation 4. Since we assume  $g$  is a differentiable function (typically implemented as a neural network), the gradient of the SSD w.r.t. each singleton centroid (keeping the weights of  $g$  fixed) can be computed easily. Over the course of the alternation, CKM can dynamically infer which clusters are singletons and which are compositional, as well as the centroid locations of the singleton clusters so as to trade off between fitting the singleton clusters and fitting the compositional clusters well. See Algorithm 3 for details. Note that (like with classic  $k$ -means) the initialization in step 1 can affect which local minimum is reached, and thus it is often useful to try multiple random seeds and to choose the best seed based on the lowest SSD.

---

**Algorithm 3** Compositional  $k$ -means (CKM)

---

**CKM**( $\mathcal{X}, \mathcal{K}, \epsilon$ ):

Set each  $m_{\{j\}}, j \in [k]$  to a randomly drawn (without replacement) example in  $\mathcal{X}$ .

Compute compositional centroids:  $m_\eta \leftarrow g(\{m_{\{j\}}\}_{j \in \eta}) \quad \forall \eta \in \mathcal{K} : |\eta| > 1$ .

**while** not converged **do**

$c_i \leftarrow \arg \min_{\eta \in \mathcal{K}} \|x_i - m_\eta\|^2 \quad \forall i$ .

$m_{\{1\}}, \dots, m_{\{k\}} \leftarrow \text{SGD}(\sum_{i=1}^n \|x_i - m_{c_i}\|^2; \{m_{\{j\}}\}_{j=1}^k; \epsilon)$

**end while**

**return**  $\{c_i\}_{i=1}^n$

---

**Convergence:** Unlike in classical  $k$ -means, the second step of the alternation (adjustment of cluster centroids) in CKM is conducted numerically rather than analytically. However, assuming the learning rate of gradient descent is sufficiently small, it will not increase the SSD. Since the first step of the alternation can also never increase the SSD, and since the SSD is bounded below, the algorithm will converge to a local minimum.

**Comparison to CAP:** CKM requires that  $g$  be differentiable, and it uses gradient-based optimization using neural network packages such as TensorFlow, PyTorch, etc. In contrast, CAP, as it only involves computing maxes and sums, can be implemented in simple Python or C code, and it does not require a differentiable  $g$ . Each step of the while-loop takes runtime  $O(nk^d)$ , where  $d$  is the size of the largest composition in  $\mathcal{K}$ . Since the number of singleton clusters  $k$  is typically much smaller than the number of examples  $n$ , CKM can run much faster than CAP.

## 5. Approach III: Greedy Compositional Reassignment (GCR)

The third approach that we explored for compositional clustering is based on the idea of using any standard clustering algorithm to partition the data  $\mathcal{X}$  into clusters, and then using the composition function  $g$  to find the optimal “reassignment” of the inferred clusters so that some of them are considered to be compositions of others. Suppose we first obtain (e.g., from Agglomerative Clustering) a set  $\mathcal{E} = \{m_{\{1\}}, \dots, m_{\{k\}}\}$  of  $k$  cluster centroids. Then we could iterate over every possible subset  $\tilde{\mathcal{E}} \subseteq \mathcal{E}$ ; these represent the compositional clusters. For each  $\tilde{\mathcal{E}}$ , we conduct an inner-loop to iterate over every possible 1-to-1 map from  $\tilde{\mathcal{E}}$  to the set of compositions (via  $g$ ) of  $\mathcal{E} \setminus \tilde{\mathcal{E}}$ ; these are the singleton/singleton clusters. We would finally select  $\tilde{\mathcal{E}}$  and its map to  $\mathcal{E} \setminus \tilde{\mathcal{E}}$  so as to minimize the sum of distances between the examples and their assigned cluster centroids (either singletons or compositional).

Unfortunately, due to the factorial time cost, this brute-force approach quickly becomes completely impractical (e.g., for  $|\mathcal{E}| = 15$  and  $d = 2$ , there are 107770296705436 possibilities; see Appendix D). However, the idea gave us inspiration for a tractable greedy heuristic that we call Greedy Compositional Reassignment (GCR). Like CKM, GCR is a centroid-based clustering method. It uses  $g$  and the distances between cluster centroids to determine the compositional relationships in a greedy manner and thereby avoid the factorial time cost. It is also constrained to find compositions of size at most 2, which is limiting in some cases but still useful in others (e.g., many natural conversations contain simultaneous speech from at most 2 speakers).

### 5.1. Procedure: Greedy Compositional Reassignment

Assume that a standard clustering method (we use Agglomerative Clustering) has produced a clustering with  $k$  centroids  $m_{\{1\}}, \dots, m_{\{k\}}$  and cluster assignments  $c_1, \dots, c_n$ , where each  $c_i \in [k]$ . Let  $\mathcal{K}$  be the set of compositions under consideration, with the restriction that  $|\eta| \leq 2$  for every  $\eta \in \mathcal{K}$ . GCR first uses  $g$  to compute the location of the compositional centroid for every  $\eta \in \mathcal{K}$  s.t.  $|\eta| = 2$ . It then finds, for each putative singleton cluster  $j \in [k]$ , the distance  $d_j$  to the closest compositional centroid  $b_j \in \mathcal{K}$ ; if  $d_j$  is below a threshold  $\tau$ , then cluster  $j$  is concluded to actually be a composition of the two other clusters in  $b_j$ , and all the examples that were previously assigned to cluster  $j$

are reassigned to the compositional cluster  $b_j$ . The process is repeated for each singleton cluster  $j$  according to the distances  $d_j$  sorted from smallest to largest until one of several possible termination conditions are reached (so as to maintain consistency, e.g., avoid cycles of compositionality); once this point is reached, all the remaining clusters that were not reassigned to be compositional are deemed to be singletons. The algorithm uses sets  $\mathcal{S}$  and  $\mathcal{T}$  to keep track of which clusters have been assigned as singletons and which are assigned as compositions, respectively. The final assignment of an example to a cluster index is denoted  $c'_i \in \mathcal{K}$  for each example  $i \in [n]$ . See Algorithm 4 for details.

---

**Algorithm 4** Greedy Compositional Reassignment (GCR)

---

```

GCR( $\mathcal{X}, \mathcal{K}, \tau$ ):
   $\mathcal{S} \leftarrow \emptyset, \mathcal{T} \leftarrow \emptyset.$ 
  Obtain preliminary clustering:  $\{m_{\{j\}}\}_{j=1}^k, \{c_i\}_{i=1}^n \leftarrow \text{AgglomerativeClustering}(\mathcal{X}).$ 
  Compute compositional centroids:  $m_\eta \leftarrow g(\{m_{\{j\}}\}_{j \in \eta}) \quad \forall \eta \in \mathcal{K}, |\eta| = 2.$ 
   $b_j \leftarrow \arg \min_{\eta:|\eta|=2} \|m_{\{j\}} - m_\eta\| \quad \forall j \in [k].$ 
   $d_j \leftarrow \|m_{\{j\}} - m_{c_j}\| \quad \forall j \in [k].$ 
  for  $j \in [k]$  according to argsort( $\{d_j\}$ ) do
    if  $d_j \geq \tau$  or  $j \in \mathcal{S}$  or  $b_j \cap \mathcal{T} \neq \emptyset$  then
      Assign remaining clusters  $j' > j$  to singletons:  $c'_i \leftarrow \{j'\} \quad \forall i : c_i = j', j' \geq j.$ 
      break
    end if
    Assign cluster  $j$  to composition:  $c'_i \leftarrow b_j \quad \forall i : c_i = j.$ 
     $\mathcal{S} \leftarrow \mathcal{S} \cup b_j.$ 
     $\mathcal{T} \leftarrow \mathcal{T} \cup \{j\}.$ 
  end for
  return  $\{c'_i\}_{i=1}^n.$ 

```

---

**Comparison to CAP and CKM:** Excluding the runtime cost of the initial clustering using Agglomerative Clustering, the GCR method is much faster than both CAP and CKM since it iterates over each of the  $k$  singleton clusters at most once, and each iteration is very simple. In contrast to the other methods, GCR is limited to compositions of size at most 2; on the other hand, this is arguably the most common case in speaker diarization anyhow (i.e., at most two people speaking simultaneously in a conversation). Note also that, whereas CKM and CAP can use the compositionality to partition the data into clusters more cleanly (see the right half of Figure 1), GCR cannot – it only has the ability to infer the compositional relationships among already-formed clusters (left half of Figure 1).

## 6. Experiments

To evaluate the proposed compositional clustering models, we conducted clustering experiments, using standard datasets that are widely used for few-shot learning research, on both multi-object image recognition and multi-person speaker diarization with overlapping speech. We follow the general workflow described in the Introduction, i.e., for each problem domain, we use few-shot learning to train an embedding function  $f^{\text{emb}}$  to separate examples by their classes, as well as a composition function  $g$  [1, 17] that can estimate the location in the embedding space of the union of two sets of classes. We train these models jointly and episodically, where each episode contains examples from a different set of classes. Before describing our experiments, we first need to define a new evaluation metric that can model the different aspects of the compositional clustering problem, and also describe the baseline methods we used for comparison.

### 6.1. Evaluation Metric: the Compositional Rand Index (CRI)

Suppose that dataset  $\mathcal{X} = \{x_1, \dots, x_n\}$  contains  $l$  singleton clusters as well as some number (possibly 0) of compositional clusters. Then  $\mathcal{Y} = 2^{[l]} \setminus \emptyset$  is the set of all possible ground-truth cluster labels, and  $y_1, \dots, y_n \in \mathcal{Y}$  are the specific cluster assignments. A sensible evaluation criterion of some inferred labels  $c_1, \dots, c_n \in \mathcal{C}$  w.r.t. the ground-truth should capture the *number* of clusters, their *purity*, and the *compositional relationships* between them. It should *not* depend on the particular naming of cluster labels (the identifiability issue). With these goals in mind, we propose the Compositional Rand Index (CRI) to compute the probability, over all pairs  $i \neq j$ , that the inferred labels agree with the ground-truth about whether the cluster assignment of example  $i$  subsumes the cluster assignment of example  $j$ :

$$\text{CRI}(c_1, \dots, c_n, y_1, \dots, y_n) = \frac{1}{n(n-1)} \sum_{i \neq j} \mathbb{I}[\mathbb{I}[c_i \supseteq c_j] = \mathbb{I}[y_i \supseteq y_j]] \quad (5)$$

where  $\mathbb{I}[\cdot]$  is a 0-1 indicator function. For datasets without compositionality (i.e.,  $\mathcal{Y} = [l]$ ), CRI is equivalent to the standard Rand Index [24].

### 6.2. Baseline Methods

Since, to our best knowledge, this clustering problem is new, it was not obvious to which baseline methods we should compare the proposed clustering methods. In the end,

we chose several baseline methods based on what seemed the most reasonable alternative approaches even if they had no explicit ability to represent compositionality among clusters. We considered several approaches:

**Ignore compositionality:** One approach is simply to ignore the compositional relationships among clusters and consider each cluster as completely independent; this is illustrated in Figure 1 (top row). Any standard clustering method can thus be used. While it will pay a penalty under the CRI metric since it misses the compositional relationships, it can sometimes (Figure 1 upper-left, but not upper-right) still do a good job overall by correctly forming coherent clusters. With this motivation, we use standard **Affinity Propagation (AP)** as well as **Agglomerative Clustering (AC)** with the Ward criterion as two baselines.

**Infer compositionality from “soft” label assignments:** Mixture models such as the classic Mixture of Gaussians and fuzzy  $k$ -means [3] (it is more commonly called “fuzzy  $c$ -means” in the literature) assign to each example a vector of probabilities that express the likelihood that it belongs to each of the  $k$  clusters. By thresholding these probabilities with some threshold  $\tau$ , one can obtain a *set* of cluster labels for each example. This method can work if the embedding space is structured so that examples whose cluster label set is  $\{a, b\}$  lie near the midpoint between those examples whose label set is  $\{a\}$  and those whose label set is  $\{b\}$ . Based on this approach, we tested both **Fuzzy  $c$ -Means (FCM)** and **Gaussian Mixture Models (GMM)** as baselines.

**Oracle singleton clustering:** To get a sense of how well a *perfect* clustering method would work that can determine the cluster memberships exactly but not infer any compositional relationships, we also include an Oracle Singleton Clustering (OSC) in our experiments.

### 6.3. Experiment I: LibriSpeech

Real-world conversations and meetings often contain moments when multiple people are speaking simultaneously (due to interruptions, sub-group conversations, etc.). Hence, an important few-shot learning problem is to identify the *set* of people speaking at any given moment in time, where the classes (people) at test time usually differ from the classes at training time. We thus used the LibriSpeech [22] dataset to explore how well each clustering method can cluster speech samples into speaker sets and infer the

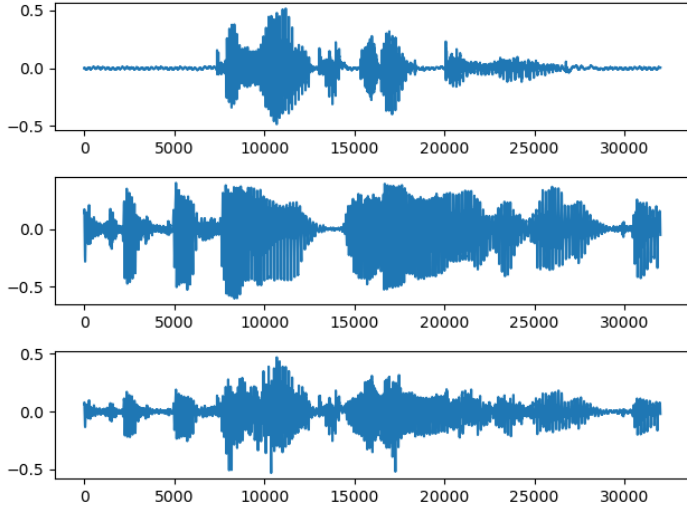


Figure 2: Some audio examples from LibriSpeech. From top to bottom are the waveforms from speaker 1, speaker 2, and overlapped speech from both speakers.

compositional relationships between sets. LibriSpeech is a corpus of approximately 1000 hours of English audiobook speech from 2484 speakers. While it contains only individual speakers, we can synthesize simultaneous speech by combining individual tracks, similarly to work by [13, 19]. See Figure 2 for some examples of the audio waveforms.

**Embedding model:** We used LibriSpeech to train a compositional embedding model ( $f^{\text{emb}}$  and  $g$ ) for speaker verification using an LSTM neural network on top of MFCC audio features (see Appendices for details). Importantly, none of the classes (speakers) that were used for optimizing these networks were used in the clustering experiments. <sup>1</sup>

**Procedure:** We created datasets  $\mathcal{X}$  of size  $n \in \{150, 750, 1500, 7500, 15000\}$ ; each dataset contained speech segments from 5 different speakers (picked from 100 speakers which were not seen during training). Some of the segments contained single speakers, and some contained combinations of two speakers (i.e.,  $d = 2$ ). Hence, there were  $\binom{5}{1} + \binom{5}{2} = 15$  different unique speaker sets in total. The test set contains 10 data trials for each  $n$  and the validation set has 10 trials when  $n = 150$  (hyperparameters are picked based on

---

<sup>1</sup>For the baseline clustering methods, we also tried training a simpler embedding model  $f^{\text{emb}}$  *without* jointly training  $g$  to check whether that gave better performance. However, we found that this actually resulted in worse performance for the baselines, and hence we abandoned it.

$n = 150$  and used for all  $ns$ ). For each  $n$ , we compared all three compositional clustering algorithms and all the baselines described above and then compared the resulting CRI scores (Section 6.1). For CAP, we used the full inference procedure for  $n = 150$ , and we used  $CAP \subset$  with a random subset of 150 examples for  $n > 150$ . All results of all clustering methods are averaged over 10 trials for each  $n$ .

**Hyperparameter optimization:** CAP,  $CAP \subset$ , and AP have one hyperparameter, which is the cost  $\gamma$  of creating a new singleton cluster. GCR has two hyperparameters: the first is the number of clusters in the first step of clustering and the second is the threshold  $\tau$  to stop compositional label assignment. CKM has four hyperparameters: the number of singleton clusters  $k$ ; the number of random initializations; the maximum number of alternations; and the learning rate. AC uses a distance threshold hyperparameter that determines whether to merge two clusters. GMM has one hyperparameter to decide the number of components. FCM has the number of clusters  $c$  and the corresponding threshold  $1/c$  on the vector of probabilities that determines when the model infers that an example belongs to a compositional cluster; it also has a temperature  $m$  that can make the estimated class probabilities more or less entropic. The hyperparameter sets were decided separately for each method, based on pilot exploration, to give each method a good chance of succeeding. The hyperparameter values were then optimized so as to maximize the average (over 10 trials) accuracy (see Appendices). Experiments were conducted using the Python code in the Supp. Materials; the sklearn implementations of `AgglomerativeClustering` and `AffinityPropagation`; and the `SciKit-Fuzzy` of FCM.

**Results:** The mean CRI% (along with standard error) are shown in Table 1. For all values of  $n$ , the compositional clustering algorithms (the first three lines of the table) worked best. The GCR usually gave the highest accuracy of the three, except for  $n = 150$ , where CKM was superior. CAP comes in second place for  $n = 150$  but as  $n$  increases, its accuracy decreases; this is likely because, for the larger  $n$  values,  $CAP \subset$  sees a relatively smaller fraction of the total dataset as  $n$  increases.

All the proposed methods outperformed the Oracle Singleton Clustering baseline, suggesting that they can both form coherent clusters and correctly infer the compositional relationships between them. Among the traditional clustering methods, FCM usually performed best: while it does have some ability to infer compositionality via the proba-

## LibriSpeech Experiments

$n$	150	750	1500	7500	15000
GCR	94.4 (1.0)	<b>95.7 (0.7)</b>	<b>95.7 (0.7)</b>	<b>96.2 (0.6)</b>	<b>96.2 (0.5)</b>
CAP	94.8 (1.4)	93.8 (1.4)	93.7 (1.5)	93.4 (1.3)	92.6 (2.1)
CKM	<b>95.8 (0.8)</b>	94.6 (1.0)	94.9 (0.8)	94.6 (0.8)	94.3 (0.9)
AP	87.9 (0.6)	87.0 (0.2)	86.1 (0.1)	85.0 (0.1)	84.8 (0.0)
AC	88.4 (0.3)	86.4 (0.2)	85.6 (0.1)	84.7 (0.0)	84.6 (0.0)
FCM	88.0 (0.5)	88.3 (0.5)	88.0 (0.4)	88.4 (0.4)	88.4 (0.4)
GMM	88.3 (0.4)	87.9 (0.6)	86.6 (0.8)	80.9 (1.4)	79.9 (1.8)
<i>OSC</i>	<i>91.1 (0.0)</i>				

Table 1: LibriSpeech results (mean CRI% and s.e.).

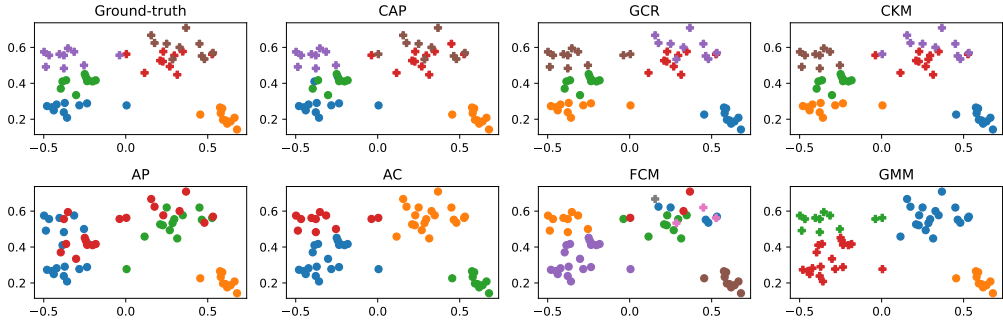


Figure 3: Some LibriSpeech clusters, according to different algorithms. Circles belong to singleton clusters; plusses belong to compositional clusters. Best viewed in color.

bility vector assigned to each example, it does not make use of the embedding model’s composition function  $g$ ; hence, it must rely solely on compositional clusters lying close to their constituent singleton clusters in the embedding space, which does not always happen in practice.

**Inferred Clusters:** Figure 3 shows some clustering results of the 4 different methods; in each plot (generated using PCA applied to  $\mathcal{X}$ ), circles and plusses represent examples from singleton and compositional clusters, respectively. (To avoid clutter, we show just 3 singleton clusters and their compositions, and the inferred relationships of which clusters are composed to yield other clusters are not shown.) All three compositional clustering methods are largely successful in inferring both the clusters and their compositionality.

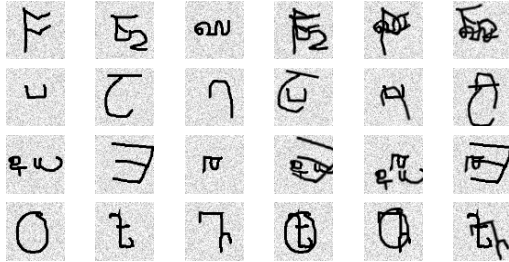


Figure 4: Some representative examples from OmniGlot images: the first three columns show examples from singleton clusters, whereas the latter show images from compositional clusters.

AP and AC can approximately infer the clusters but sometimes lump groups of examples together that actually come from distinct clusters. FCM and GMM do manage to infer some compositionality correctly, but not as well as the compositional methods.

#### 6.4. Experiment II: OmniGlot

Here we considered a multi-object image recognition problem using the OmniGlot [15] dataset. The OmniGlot dataset contains images of handwritten symbols from a variety of languages. It has 1623 different handwritten characters from 50 different alphabets. We can synthesize images with multiple symbols by element-wise superposition; Figure 4 shows 4 groups of examples used in the experiment, where each group contains images with cluster labels  $\{1\}$ ,  $\{2\}$ ,  $\{3\}$ ,  $\{1, 2\}$ ,  $\{1, 3\}$ ,  $\{2, 3\}$ . Because of the intertwining of the different symbols in each compositional image, the recognition problem is quite challenging even for humans.

In this experiment, we also created 10 trials for each  $n$  in the test set and 10 trials when  $n = 150$  in the validation set.

**Embedding model:** In our experiment, all characters are augmented with random scaling and shifting, and random Gaussian noise is added to the background. We pre-trained a compositional embedding model  $f^{\text{emb}}$  using a ResNet18 [12] network; the composition function  $g$  is the same as for LibriSpeech (see Appendices).

**Procedures and hyperparameter optimization:** The procedures are analogous to the experiments on LibriSpeech (see Section 6.3).

**Results:** Mean CRI% (and standard errors) are in Table 2. On this dataset, CKM gave the highest accuracy for all values of  $n$ . With CKM (both on LibriSpeech and

**OmniGlot Experiments**

<i>n</i>	150	750	1500	7500	15000
GCR	94.9 (0.4)	95.9 (0.3)	96.0 (0.2)	96.3 (0.3)	96.3 (0.3)
CAP	93.3 (0.4)	92.8 (0.5)	92.6 (0.5)	92.7 (0.4)	92.8 (0.2)
CKM	<b>96.9 (0.8)</b>	<b>97.6 (0.2)</b>	<b>97.6 (0.2)</b>	<b>97.5 (0.2)</b>	<b>97.5 (0.2)</b>
AP	87.9 (0.1)	86.3 (0.1)	85.6 (0.1)	84.8 (0.0)	84.7 (0.0)
AC	87.8 (0.1)	85.7 (0.1)	85.2 (0.0)	84.7 (0.0)	84.6 (0.0)
FCM	88.2 (0.2)	88.2 (0.1)	87.9 (0.2)	88.0 (0.2)	88.0 (0.1)
GMM	87.9 (0.2)	88.9 (0.2)	87.8 (0.4)	83.7 (0.1)	78.6 (1.7)
<i>OSC</i>	<i>91.1 (0.0)</i>				

Table 2: OmniGlot results (mean CRI% and s.e.).

OmniGlot), we found that trying different random initializations of the singleton cluster centroids, and then choosing the final clustering based on the sum of squared distances after training, was important to get good performance. Nonetheless, CKM’s accuracy was not just due to randomly “guessing” which of the clusters were singleton clusters – the number of random seeds in our experiments (we used 100) was far smaller than the total number of possible choices of 5 singleton clusters out of 15 total clusters ( $\binom{15}{5} = 3003$ ), suggesting that CKM uses  $g$  and the numerical SSD-minimization procedure to deduce compositional structure. After CKM, GCR was second best, followed by CAP. Among the traditional clustering methods, FCM usually performed best.

## 7. Conclusions

We presented three new algorithms – Compositional Affinity Propagation (CAP), Compositional  $k$ -means (CKM), and Greedy Compositional Reassignment (GCR) – that can both cluster data and infer the compositional relationships between clusters, and we showed promising results on the LibriSpeech and OmniGlot datasets for multi-speaker diarization and multi-object image recognition applications, respectively. These tools can facilitate data visualization and exploratory data analyses on datasets where the classes have not been previously seen. Our experiments with these new compositional clustering methods on these datasets suggest that modeling compositionality explicitly is useful and enables it to both identify coherent and distinctive clusters and to infer the

compositional relationship between them. In particular, these new clustering algorithms deliver substantially higher accuracy than can be achieved with standard clustering methods (e.g., GMM, FCM), even when the latter have the ability to assign examples “softly” to multiple clusters. Among CKM, GCR, and CAP, we found that CKM and GCR gave higher accuracy and also scale better with dataset size  $n$ .

**Future work:** We anticipate that, as multi-label few-shot learning research continues to grow as a field, there will be increasing interest for methods to cluster data from unseen classes automatically. Research on more accurate compositional embedding models, especially to the extent that the composition function  $g$  can be increased in accuracy, will likely lead to accuracy improvements in compositional clustering algorithms as well. Also, one downstream application of our work that would be interesting to explore is a simplified pipeline for speaker diarization: instead of separate algorithms to detect overlapping speech, separate speech segments into long vs. short turns, and then cluster the utterances [6], it may be possible to apply a compositional clustering algorithm that can diarize the set of all speech utterances in just one pass.

**Acknowledgement:** This research was supported by the NSF National AI Institute for Student-AI Teaming (iSAT) under grant DRL #2019805. The opinions expressed are those of the authors and do not represent views of the NSF. The research was also supported by NSF award #2046505.

## References

- [1] Alfassy, A., Karlinsky, L., Aides, A., Shtok, J., Harary, S., Feris, R., Giryes, R., Bronstein, A.M., 2019. Laso: Label-set operations networks for multi-label few-shot learning, in: Proceedings of the IEEE/CVF Conference on Computer Vision and Pattern Recognition, pp. 6548–6557.
- [2] Allen, C., Hospedales, T., 2019. Analogies explained: Towards understanding word embeddings, in: International Conference on Machine Learning, PMLR. pp. 223–231.
- [3] Bezdek, J.C., Ehrlich, R., Full, W., 1984. Fcm: The fuzzy c-means clustering algorithm. Computers & geosciences 10, 191–203.
- [4] Bickel, S., Scheffer, T., 2004. Multi-view clustering., in: ICDM, Citeseer. pp. 19–26.
- [5] Blei, D.M., Jordan, M.I., 2006. Variational inference for dirichlet process mixtures. Bayesian analysis 1, 121–143.
- [6] Bullock, L., Bredin, H., Garcia-Perera, L.P., 2020. Overlap-aware diarization: Resegmentation using neural end-to-end overlapped speech detection, in: ICASSP 2020-2020 IEEE International Conference on Acoustics, Speech and Signal Processing (ICASSP), IEEE. pp. 7114–7118.
- [7] Chen, T., Lin, L., Hui, X., Chen, R., Wu, H., 2020. Knowledge-guided multi-label few-shot learning for general image recognition. IEEE Transactions on Pattern Analysis and Machine Intelligence .
- [8] Deng, J., Guo, J., Xue, N., Zafeiriou, S., 2019. Arcface: Additive angular margin loss for deep face recognition, in: Proceedings of the IEEE/CVF conference on computer vision and pattern recognition, pp. 4690–4699.
- [9] Franklin, N.T., Frank, M.J., 2018. Compositional clustering in task structure learning. PLoS computational biology 14, e1006116.

[10] Frey, B.J., Dueck, D., 2007. Clustering by passing messages between data points. *Science* 315, 972–976.

[11] Hariharan, B., Girshick, R., 2017. Low-shot visual recognition by shrinking and hallucinating features, in: Proceedings of the IEEE international conference on computer vision, pp. 3018–3027.

[12] He, K., Zhang, X., Ren, S., Sun, J., 2016. Deep residual learning for image recognition, in: Proceedings of the IEEE conference on computer vision and pattern recognition, pp. 770–778.

[13] Hershey, J.R., Chen, Z., Le Roux, J., Watanabe, S., 2016. Deep clustering: Discriminative embeddings for segmentation and separation, in: 2016 IEEE International Conference on Acoustics, Speech and Signal Processing (ICASSP), IEEE. pp. 31–35.

[14] Huynh, D., Elhamifar, E., 2021. Interaction compass: Multi-label zero-shot learning of human-object interactions via spatial relations, in: Proceedings of the IEEE/CVF International Conference on Computer Vision, pp. 8472–8483.

[15] Lake, B.M., Salakhutdinov, R., Tenenbaum, J.B., 2015. Human-level concept learning through probabilistic program induction. *Science* 350, 1332–1338.

[16] Lee, C.W., Fang, W., Yeh, C.K., Wang, Y.C.F., 2018. Multi-label zero-shot learning with structured knowledge graphs, in: Proceedings of the IEEE conference on computer vision and pattern recognition, pp. 1576–1585.

[17] Li, Z., Mozer, M., Whitehill, J., 2021. Compositional embeddings for multi-label one-shot learning, in: Proceedings of the IEEE/CVF Winter Conference on Applications of Computer Vision, pp. 296–304.

[18] Li, Z., Whitehill, J., 2021. Compositional embedding models for speaker identification and diarization with simultaneous speech from 2+ speakers, in: ICASSP 2021-2021 IEEE International Conference on Acoustics, Speech and Signal Processing (ICASSP), IEEE. pp. 7163–7167.

[19] Menne, T., Sklyar, I., Schlüter, R., Ney, H., 2019. Analysis of deep clustering as preprocessing for automatic speech recognition of sparsely overlapping speech. *arXiv preprint arXiv:1905.03500* .

[20] Miller, G.A., 1995. Wordnet: a lexical database for english. *Communications of the ACM* 38, 39–41.

[21] Narayan, S., Gupta, A., Khan, S., Khan, F.S., Shao, L., Shah, M., 2021. Discriminative region-based multi-label zero-shot learning, in: Proceedings of the IEEE/CVF International Conference on Computer Vision, pp. 8731–8740.

[22] Panayotov, V., Chen, G., Povey, D., Khudanpur, S., 2015. Librispeech: an asr corpus based on public domain audio books, in: 2015 IEEE international conference on acoustics, speech and signal processing (ICASSP), IEEE. pp. 5206–5210.

[23] Pennington, J., Socher, R., Manning, C.D., 2014. Glove: Global vectors for word representation, in: Proceedings of the 2014 conference on empirical methods in natural language processing (EMNLP), pp. 1532–1543.

[24] Rand, W.M., 1971. Objective criteria for the evaluation of clustering methods. *Journal of the American Statistical association* 66, 846–850.

[25] Schroff, F., Kalenichenko, D., Philbin, J., 2015. Facenet: A unified embedding for face recognition and clustering, in: Proceedings of the IEEE conference on computer vision and pattern recognition, pp. 815–823.

[26] Snyder, D., Garcia-Romero, D., Sell, G., Povey, D., Khudanpur, S., 2018. X-vectors: Robust dnn embeddings for speaker recognition, in: 2018 IEEE International Conference on Acoustics, Speech and Signal Processing (ICASSP), IEEE. pp. 5329–5333.

[27] Song, G., Tan, X., Zhao, J., Yang, M., 2021. Deep robust multilevel semantic hashing for multi-label cross-modal retrieval. *Pattern Recognition* 120, 108084.

[28] Ward Jr, J.H., 1963. Hierarchical grouping to optimize an objective function. *Journal of the American statistical association* 58, 236–244.

[29] Weiss, Y., Freeman, W.T., 2001. On the optimality of solutions of the max-product belief-propagation algorithm in arbitrary graphs. *IEEE Transactions on Information Theory* 47, 736–744.

[30] Yin, R., Bredin, H., Barras, C., 2018. Neural speech turn segmentation and affinity propagation for speaker diarization, in: Annual Conference of the International Speech Communication Association.

[31] Zelenak, M., Segura, C., Luque, J., Hernando, J., 2012. Simultaneous speech detection with spatial features for speaker diarization. *IEEE Transactions on Audio, Speech, and Language Processing* 20, 436–446.

[32] Zhou, F., Huang, S., Liu, B., Yang, D., 2021. Multi-label image classification via category prototype compositional learning. *IEEE Transactions on Circuits and Systems for Video Technology* .

## Appendix A. Data and Code

The data and code are available in the following Google Drive folder: <https://drive.google.com/drive/folders/15YDeik6gIQrL3A1ow--9a86QTjZ513gR>

For the OmniGlot and LibriSpeech experiments, run the `run.sh` commands.

## Appendix B. Loopy Belief Propagation for Standard Affinity Propagation

When applying the max-product algorithm (a technique to find MAP estimates using loopy belief propagation) to the factor graph shown in the main paper for standard Affinity Propagation, a sequence of “messages” (functions  $\alpha, \rho : [n] \times [n] \times \mathcal{C} \rightarrow \mathbb{R}_{\leq 0} \cup \{-\infty\}$ ) is passed back and forth between the variable and factor nodes. Each variable  $i$  sends a message  $\rho_{i \rightarrow k}(c_i)$  to constraint  $k$ , and each constraint  $k$  sends a message  $\alpha_{i \leftarrow k}(c_i)$  to variable  $i$ , about the likelihood of each possible value of  $c_i$ .

The max-sum algorithm (and the related max-product algorithm for factor graphs) dictates that  $\rho_{i \rightarrow k}(c_i)$  equals the sum of messages over  $c_i$ ’s neighbors *except*  $\delta_k$  (i.e.,  $\{\delta_{k'}\}_{k' \neq k}$ ):

$$\rho_{i \rightarrow k}(c_i) = S(i, c_i) + \sum_{k' \neq k} \alpha_{i \leftarrow k'}(c_i) \quad (\text{B.1})$$

Also, for MAP estimation,  $\alpha_{i \leftarrow k}(c_i)$  equals the maximum possible sum of the messages from all of  $\delta_k$ ’s neighbors *except*  $i$  (i.e.,  $\{c_{i'}\}_{i' \neq i}$ ), plus the value of  $\delta_k$  itself:

$$\alpha_{i \leftarrow k}(c_i) = \max_{\{c_{i'}\}_{i' \neq i}} \left[ \delta_k(c_1, \dots, c_n) + \sum_{i' \neq i} \rho_{i' \rightarrow k}(c_{i'}) \right] \quad (\text{B.2})$$

## Appendix C. Derivation of Algorithm 1 (CAP) and Proof of Theorem 1

In this Appendices we derive Algorithm 1 from the definitions of  $\alpha$  and  $\rho$  in the message passing algorithm to optimize the Compositional Affinity Propagation model described in the main paper. We also prove the time cost in Theorem 1.

Recall the definitions of  $\alpha$ ,  $\rho$ , and  $\delta$ :

$$\rho_{i \rightarrow k}(c_i) = S(i, c_i) + \sum_{k' \neq k} \alpha_{i \leftarrow k'}(c_i) \quad (\text{C.1})$$

$$\alpha_{i \leftarrow k}(c_i) = \max_{\{c_{i'}\}_{i' \neq i}} \left[ \delta_k(c_1, \dots, c_n) + \sum_{i' \neq i} \rho_{i' \rightarrow k}(c_{i'}) \right] \quad (\text{C.2})$$

$$\delta_k(c_1, \dots, c_n) = \begin{cases} -\infty & \text{if } \exists i : (c_i \ni k) \wedge (c_k \neq \{k\}) \\ 0 & \text{otherwise} \end{cases} \quad (\text{C.3})$$

Each message  $\alpha_{i \leftarrow k}(c_i)$  computes, for a given value of  $c_i$  for variable  $i$ , an (unnormalized) log-likelihood of the *best possible configuration* of the assignments of all the *other* variables  $\{c_{i' \neq i}\}$ , given that constraint  $k$  is satisfied (i.e.,  $\delta_k$  is finite). There are four cases in which this occurs; they mirror those in standard Affinity Propagation but differ slightly. For each case, the  $\delta$  term in the RHS of Eqn. C.2 vanishes; the only remaining terms are the sum of the  $\rho$ 's. Also, since each summand in Eqn. C.2 depends on just a single unique  $c_{i'}$ , the max of the sum becomes the sum of the max. Cases:

1.  $i = k, c_i = \{k\}$ : Since in this case example  $i = k$  designates itself as an exemplar, then the constraint  $\delta_k$  is immediately satisfied. Moreover, any of the other examples  $i' \neq i$  is free to choose (or not choose) example  $k$  as an exemplar, and therefore we can take the maximum over *any* possible value for each  $c_{i'}$ . Hence,

$$\begin{aligned} \alpha_{i \leftarrow k}(c_i) &= \max_{\{c_{i'}\}_{i' \neq k}} \left[ 0 + \sum_{i' \neq k} \rho_{i' \rightarrow k}(c_{i'}) \right] \\ &= \sum_{i' \neq k} \max_{c_{i'}} \rho_{i' \rightarrow k}(c_{i'}) \end{aligned}$$

2.  $i = k, c_i \not\ni k$ : Since example  $i = k$  does not designate itself as an exemplar, then none of the other examples  $i' \neq i$  may choose  $k$  as its exemplar. Hence,  $\alpha_{i \leftarrow k}(c_i) = \sum_{i' \neq k} \max_{c_{i'} \not\ni k} \rho_{i' \rightarrow k}(c_{i'})$ .
3.  $i \neq k, c_i \ni k$ : Since example  $i$  designates its exemplar either to be or to include example  $k$ , then  $\alpha$  is finite only if  $c_k = \{k\}$ , and each remaining example  $i' \notin \{i, k\}$  is free to designate any example as its exemplar. Hence,  $\alpha_{i \leftarrow k}(c_i) = \rho_{k \rightarrow k}(\{k\}) + \sum_{i' \notin \{i, k\}} \max_{c_{i'}} \rho_{i' \rightarrow k}(c_{i'})$ .
4.  $i \neq k, c_k \not\ni k$ : Since example  $i$  does not designate  $k$  as an exemplar, then example  $k$  is free either to be an exemplar or not, and we must take the max over both

possibilities:

$$\alpha_{i \leftarrow k}(c_i) = \max \left[ \max_{c_k \not\in k} \rho_{k \rightarrow k}(c_k) + \sum_{i' \notin \{i, k\}} \max_{c_{i'} \not\in k} \rho_{i' \rightarrow k}(c_{i'}), \rho_{k \rightarrow k}(\{k\}) + \sum_{i' \notin \{i, k\}} \max_{c_{i'}} \rho_{i' \rightarrow k}(c_{i'}) \right]$$

Note that  $\alpha_{i \leftarrow k}(c_i) = -\infty$  if  $i = k$ ,  $c_i \ni i$  and  $c_i \neq \{i\}$ . However, in practice we can avoid this case by instead setting  $S(i, c_i) = -\infty$  whenever  $c_i \ni i$  and  $c_i \neq \{i\}$ .

Given the four cases above, we have the following definition of  $\alpha$ :

$$\alpha_{i \leftarrow k}(c_i) = \max_{\{c_{i'}\}_{i' \neq i}} \left[ \delta_k(c_1, \dots, c_n) + \sum_{i' \neq i} \rho_{i' \rightarrow k}(c_{i'}) \right] \quad (\text{C.4})$$

$$= \begin{cases} \sum_{i' \neq k} \max_{c_{i'}} \rho_{i' \rightarrow k}(c_{i'}) & i = k, c_i = \{k\} \\ \sum_{i' \neq k} \max_{c_{i'} \not\in k} \rho_{i' \rightarrow k}(c_{i'}) & i = k, c_i \not\ni k \\ \rho_{k \rightarrow k}(k) + \sum_{i' \notin \{i, k\}} \max_{c_{i'}} \rho_{i' \rightarrow k}(c_{i'}) & i \neq k, c_i \ni \{k\} \\ \max \left[ \max_{c_k \not\in k} \rho_{k \rightarrow k}(c_k) + \sum_{i' \notin \{i, k\}} \max_{c_{i'} \not\in k} \rho_{i' \rightarrow k}(c_{i'}), \rho_{k \rightarrow k}(k) + \sum_{i' \notin \{i, k\}} \max_{c_{i'}} \rho_{i' \rightarrow k}(c_{i'}) \right] & i \neq k, c_k \not\ni k \end{cases} \quad (\text{C.5})$$

In the most naive implementation, evaluating  $\alpha$  for *each* tuple  $(i, k, c_i)$  would take time  $O(n^2)$  due to the summing over the max; the entire table of  $\alpha$  values would thus take time  $O(n^4 \times |\mathcal{C}|)$ . However, there is massive redundancy that can be avoided: First, for each tuple  $(i, k)$ , only two possible values of  $\alpha_{i \leftarrow k}(c_i)$  exist: one for  $c_i \ni k$  (i.e.,  $\alpha_{i \leftarrow k}(\phi(k))$ ) and one for  $c_i \not\ni k$  (i.e.,  $\alpha_{i \leftarrow k}(\bar{\phi}(k))$ ). Hence, instead of computing  $|\mathcal{C}|$  values for each tuple  $(i, k)$ , we need to compute and store only 2 values. Second, the expressions  $\sum_{i' \neq k} \max_{c_{i'}} \rho_{i' \rightarrow k}(c_{i'})$  and  $\sum_{i' \neq k} \max_{c_{i'} \not\in k} \rho_{i' \rightarrow k}(c_{i'})$  depend on  $k$  but not on  $i$ ; hence, they can be reused for many tuples  $(i, k)$ . Third:

$$\begin{aligned} \sum_{i' \notin \{i, k\}} \max_{c_{i'}} \rho_{i' \rightarrow k}(c_{i'}) &= \sum_{i' \neq k} \max_{c_{i'}} \rho_{i' \rightarrow k}(c_{i'}) - \max_{c_i} \rho_{i \rightarrow k}(c_i) \\ \sum_{i' \notin \{i, k\}} \max_{c_{i'} \not\in k} \rho_{i' \rightarrow k}(c_{i'}) &= \sum_{i' \neq k} \max_{c_{i'} \not\in k} \rho_{i' \rightarrow k}(c_{i'}) - \max_{c_i \not\in k} \rho_{i \rightarrow k}(c_i) \end{aligned}$$

Hence, after computing each of the terms of the LHS above (just once for each  $k$ ), we need only to “adjust” them for each  $i$ , in  $O(1)$  time, by subtracting the corresponding term on the RHS.

At the end of all the CAP iterations, we set

$$c_i^{\text{MAP}} = \arg \max_{c_i} \left[ \sum_k \alpha_{i \leftarrow k}(c_i) + S(i, c_i) \right]$$

Hence, as long as we can update  $\alpha$  during each iteration of message passing, then we never need to know  $\rho$  explicitly.

For convenience, define the following functions:

$$\begin{aligned}
b(i, k) &= \max_{c_i} \rho_{i \rightarrow k}(c_i) \\
\bar{b}(i, k) &= \max_{c_i \not\in k} \rho_{i \rightarrow k}(c_i) \\
e(k) &= \sum_{i' \neq k} \max_{c_{i'}} \rho_{i' \rightarrow k}(c_{i'}) = \sum_{i' \neq k} b(i', k) \\
\bar{e}(k) &= \sum_{i' \neq k} \max_{c_{i'} \not\in k} \rho_{i' \rightarrow k}(c_{i'}) = \sum_{i' \neq k} \bar{b}(i', k) \\
h(k) &= \rho_{k \rightarrow k}(k) \\
a(i, k) &= \alpha_{i \leftarrow k}(\phi(k)) = \begin{cases} e(k) & i = k \\ h(k) + e(k) - b(i, k) & i \neq k \end{cases} \\
\bar{a}(i, k) &= \alpha_{i \leftarrow k}(\bar{\phi}(k)) = \begin{cases} \bar{e}(k) & i = k \\ \max(\bar{b}(k, k) + \bar{e}(k) - \bar{b}(i, k), h(k) + e(k) - b(i, k)) & i \neq k \end{cases}
\end{aligned}$$

Visual inspection of Equation C.5 confirms that the  $a(i, k)$  and  $\bar{a}(i, k)$  defined above recover all  $2n^2$  degrees of freedom of  $\alpha$ . Below we show how we can compute  $e, \bar{e}, b, \bar{b}$ , and  $h$  in a *total* time of  $O(dn^{d+1})$  per iteration. First, however, we need to derive the computation of some intermediate quantities.

*Appendix C.1. Computing  $q(i, c_i) = \sum_{k'} \alpha_{i \leftarrow k'}(c_i) \forall i, c_i$*

Define  $q(i, c_i) = \sum_{k'} \alpha_{i \leftarrow k'}(c_i)$ . For each  $i$ , we can compute  $q(i, c_i)$  for each  $c_i$  by splitting the sum over  $k'$  into two parts: those  $k'$  such that  $\phi(k') \ni c_i$  and those  $k'$  such that  $\bar{\phi}(k') \ni c_i$ . We then substitute  $\alpha_{i \leftarrow k'}(c_i) = \alpha_{i \leftarrow k'}(\phi(k'))$  for  $k'$  s.t.  $\phi(k') \ni c_i$  (and similarly for  $\bar{\phi}(k')$ ) to yield:

$$\begin{aligned}
q(i, c_i) &= \sum_{k': \phi(k') \ni c_i} \alpha_{i \leftarrow k'}(\phi(k')) + \sum_{k': \bar{\phi}(k') \ni c_i} \alpha_{i \leftarrow k'}(\bar{\phi}(k')) \\
&= \sum_{k'} \alpha_{i \leftarrow k'}(\bar{\phi}(k')) + \sum_{k': \phi(k') \ni c_i} (\alpha_{i \leftarrow k'}(\phi(k')) - \alpha_{i \leftarrow k'}(\bar{\phi}(k'))) \\
&= \sum_{k'} \alpha_{i \leftarrow k'}(\bar{\phi}(k')) + \sum_{k' \in c_i} (\alpha_{i \leftarrow k'}(\phi(k')) - \alpha_{i \leftarrow k'}(\bar{\phi}(k')))
\end{aligned}$$

We can define  $q^*(i) = \sum_{k'} \alpha_{i \leftarrow k'}(\bar{\phi}(k'))$ . Then we have:

$$q(i, c_i) = q^*(i) + \sum_{k' \in c_i} (a(i, k') - \bar{a}(i, k'))$$

The term  $q^*(i)$  takes time  $O(n)$  for each  $i$  but is reused for all  $c_i$ . The summation on the RHS contains at most  $d$  terms (for a maximum composition size of  $d$ ). Hence, for each  $i$ , the total computation (over all  $c_i$ ) is  $O(n + |\mathcal{C}|d) = O(n + dn^d) = O(dn^d)$ .

### Appendix C.2. Efficiently Finding Maxima of Many Subsets

The next step we need is an efficient method to compute expressions of the forms (a)  $\max_{c_i \in \phi(k)} q(i, c_i)$  and (b)  $\max_{c_i \in \bar{\phi}(k)} q(i, c_i)$  for all  $k$ , in a total time of  $O(n^{d+1})$ .

Form (a): Since each such  $c_i$  must contain  $k$ , then there are only  $d - 1$  remaining degrees of freedom for each  $\phi(k)$ ; hence,  $|\phi(k)| \leq n^{d-1}$  for each  $k$ , and directly computing the maximum of  $q(i, \cdot)$  over every  $\phi(k)$  takes a total time of  $O(n^d)$  (summed over all  $k$ ).

Form (b): Define  $\bar{\phi}^j(k) = \{c \in \bar{\phi}(k) : |c| = j\}$ . Since  $\max_{c_i \in \bar{\phi}(k)} q(i, c_i) = \max_{j \in [d]} \max_{c_i \in \bar{\phi}^j(k)} q(i, c_i)$ , we can split the task into subtasks by  $j$  and then take the max over all of them. To compute the max over each  $\bar{\phi}^j(k)$ , we can iterate over all  $n^{j-1}$  tuples  $(t_1, \dots, t_{j-1}) \in [n]^{j-1}$ ; for each tuple, we can compute in  $O(n)$  time the largest and second-largest value of  $q(i, \cdot)$  over the set  $(t_1, \dots, t_{j-1}, t_j)$  and then “adjust” the result in constant time to obtain the update for each  $k$ . In particular, for each such tuple  $\tau$ , let  $\psi_\tau = \{\{t_1, \dots, t_j\} \in \mathcal{C} : t_1 < \dots < t_j\}$ . (For instance, if  $j = 2$ ,  $n = 4$ ,  $\tau = (1, 2)$ , and  $\mathcal{C}$  contains all 3-tuples, then  $\psi_\tau = \{\{1, 2, 3\}, \{1, 2, 4\}\}$ .) In each iteration, let  $c^1, c^2 \in \psi_\tau$  be the arguments corresponding to the largest and second-largest elements in  $q(i, \psi_\tau)$ ; if  $|\psi_\tau| = 1$ , then define  $c^2 = \emptyset$ ; if  $|\psi_\tau| = 0$ , then define both  $c^1 = c^2 = \emptyset$ . (Note that  $\emptyset \notin \bar{\phi}(k)$  for any  $k$ .) For any  $k$ , it must be the case that the number of elements in the set  $\psi_\tau \cap \bar{\phi}^j(k)$  is either 0 (if any  $k \in \{t_1, \dots, t_{j-1}\}$ ),  $|\psi_\tau| - 1$  (if  $k > t_{j-1}$ , such that we must ignore exactly one element of  $\psi_\tau$  for each  $k$ ), or  $|\psi_\tau|$  (if  $k \notin \{t_1, \dots, t_{j-1}\}$  and  $k < t_{j-1}$ ). In the first case (intersection is empty), we make no update to  $\max_{c_i \in \bar{\phi}^j(k)} q(i, c_i)$ . In the second (intersection is of size  $|\psi_\tau| - 1$ ), we update  $\max_{c_i \in \bar{\phi}^j(k)} q(i, c_i)$  with  $q(i, c^1)$  if  $c^1 \not\supseteq k$  and with  $q(i, c^2)$  otherwise. And in the third (intersection is of size  $|\psi_\tau|$ ), we always update  $\max_{c_i \in \bar{\phi}^j(k)} q(i, c_i)$  with  $q(i, c^1)$ . Since  $c^1, c^2$  can be computed in time  $|\psi_\tau| \leq n$  and then reused for *each* of the  $k$  (in constant-time) for the updates, and since there are at most  $n^{j-1}$  such tuples  $\tau$  when scanning the entire  $\mathcal{C}$ , then this amounts to a total time of

$O(dn^j)$  for each  $j$ . Summing over all  $j = 1, \dots, d$ , this yields a running time of  $O(dn^d)$ . See Algorithm 2. The  $\arg \max^{1,2}$  function returns the  $c^1, c^2$  that give the largest and second-largest values of the specified function, where  $c^2 = \emptyset$  if the input set is of size 1, and  $c^1 = c^2 = \emptyset$  if the input set is empty.

### Appendix C.3. Computing Maxes of Sums Except Row $k$

We can now show how expressions of the form  $b(i', k) = \max_{c_{i'}} \rho_{i' \rightarrow k}(c_{i'})$  and  $\bar{b}(i', k) = \max_{c_{i'} \not\ni k} \rho_{i' \rightarrow k}(c_{i'})$  can be computed efficiently. We first examine the former, which by definition is:

$$\max_{c_{i'}} \rho_{i' \rightarrow k}(c_{i'}) = \max_{c_{i'}} \left[ S(i', c_{i'}) + \sum_{k' \neq k} \alpha_{i' \leftarrow k'}(c_{i'}) \right]$$

In other words, we need to find the  $c_{i'}$  that maximizes  $S(i', c_{i'})$  plus the sum (except the  $k$ th term) of the  $\alpha_{i' \leftarrow k'}(c_{i'})$  (see Figure C.5). As mentioned above, for each  $i', k$ , function  $\alpha_{i' \leftarrow k}(\cdot)$  has only 2 degrees of freedom: one for  $c_{i'} \in \phi(k)$  (the blue regions in Figure C.5) and one for  $c_{i'} \in \bar{\phi}(k)$  (the clear regions); hence, there exist numbers  $u, v$  such that  $\alpha_{i' \leftarrow k}(\phi(k)) = u$  and  $\alpha_{i' \leftarrow k}(\bar{\phi}(k)) = v$ . Assume we have already computed  $q(i, c_{i'}) = \sum_{k'} \alpha_{i' \leftarrow k'}(c_{i'}) \forall c_{i'}$  (this is the sum over *all*  $k$ ) and also, for each  $k$ , the values  $r(k) = \max_{c_{i'} \in \phi(k)} \sum_{k'} \alpha_{i' \leftarrow k'}(c_{i'})$  and  $s(k) = \max_{c_{i'} \in \bar{\phi}(k)} \sum_{k'} \alpha_{i' \leftarrow k'}(c_{i'})$ . Then, for any  $k$ , we can find, in  $O(1)$  time,  $\max_{c_{i'}} \sum_{k' \neq k} \alpha_{i' \leftarrow k'}(c_{i'})$  by “adjusting”  $\max_{c_{i'}} \sum_{k'} \alpha_{i' \leftarrow k'}(c_{i'})$  as follows:

$$\max_{c_{i'}} \sum_{k' \neq k} \alpha_{i' \leftarrow k'}(c_{i'}) = \max(r(k) - u, s(k) - v)$$

The latter case ( $\max_{c_{i'} \not\ni k} \rho_{i' \rightarrow k}(c_{i'})$ ) is even easier since we ignore all  $c_{i'} \in \phi(k)$  entirely:

$$\max_{c_{i'} \not\ni k} \sum_{k' \neq k} \alpha_{i' \leftarrow k'}(c_{i'}) = s(k) - v$$

We have already defined  $u = a(i', k)$  and  $v = \bar{a}(i', k)$ ; hence, we have:

$$\begin{aligned} b(i', k) &= \max(r(k) - a(i', k), s(k) - \bar{a}(i', k)) \\ \bar{b}(i', k) &= s(k) - \bar{a}(i', k) \end{aligned}$$

### Appendix C.4. Computing $h(k) = \rho_{k \rightarrow k}(k)$

As the last step, we can compute  $h(k) = \rho_{k \rightarrow k}(k) = S(k, \{k\}) + \sum_{k' \neq k} \alpha_{k \leftarrow k'}(k) = S(k, \{k\}) + q_k(\{k\}) - a(k, k)$ . This completes the derivation of Algorithm 1.

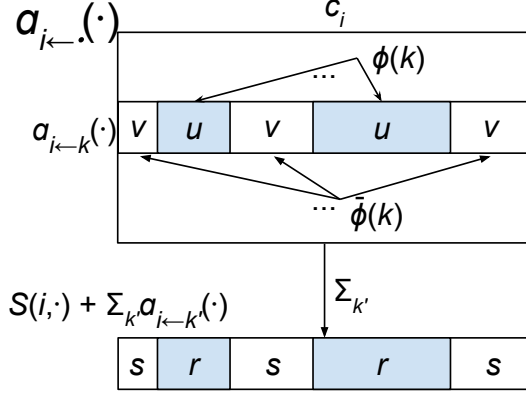


Figure C.5: For each  $i, k$ , to compute the max (over  $c_{i'}$ ) of the sum of all rows  $k' \neq k$ , we can (1) compute the max of the sum of *all* rows within region  $\phi(k)$  and (separately) within region  $\bar{\phi}(k)$ ; (2) adjust each maximum by subtracting the value of row  $k$  in region  $\phi(k)$  and the value of row  $k$  in region  $\bar{\phi}(k)$ , respectively; (3) take the larger result.

### Appendix C.5. Time Cost Analysis

As explained in Section Appendix C.2, the `FindAllMaxes` takes time  $O(dn^d)$  operations for each  $i$ . The function `ComputeRhoStats` calls `FindAllMaxes`  $n$  times (and also executes  $O(n^2)$  further operations) for a cost of  $dn^{d+1}$ . The function `ComputeAlphaStats` takes  $O(n^2)$  for the nested for-loops, and (as explained in Section Appendix C.1) a further  $O(dn^d)$  for the computation of each  $q(i, \cdot)$ , amounting to  $O(dn^{d+1})$  in total.

This completes the proof.

### Appendix D. Brute-Force Reassignment

Here is how a brute-force reassignment could work: We first obtain a set of  $k$  singleton clusters with associated exemplar indices  $\mathcal{E} \subset [n]$ . Then we iterate over every possible subset  $\tilde{\mathcal{E}} \subseteq \mathcal{E}$ ; these represent the compositional clusters. For each  $\tilde{\mathcal{E}}$ , we conduct an inner-loop to iterate over every possible 1-to-1 map from  $\tilde{\mathcal{E}}$  to the set of compositions of  $\mathcal{E} \setminus \tilde{\mathcal{E}}$ ; these represent the singleton clusters. If we consider compositions of at most  $d$  exemplars, then we have

$$\sum_{i=0}^k C(k, i) P \left( \sum_{d'=2}^d C(k - i, d'), i \right)$$

total possible maps, where  $C(k, i)$  and  $P(k, i)$  are the numbers of combinations and permutations of  $i$  objects from a set of  $k$ , respectively. The  $P$  arises due to iterating over

all 1-to-1 maps. Note that the number of possible maps grows factorially with  $k$ , and hence it quickly becomes intractable as  $k$  grows (e.g., for  $k = 15$  and  $d = 2$ , the number of possibilities is 107770296705436).

## Appendix E. LibriSpeech

LibriSpeech contains 1000+ hours of recorded English-language speech of people reading audiobooks. While the dataset contains speech from only individual speakers, we can synthesize speech by adding together the waveforms of multiple speakers. Figure 2 shows of an example of how simultaneous speech data is synthesized from LibriSpeech data.

**Compositional embedding model:** Speaker embeddings were extracted from mel-frequency cepstrum coefficient (MFCC) features (32 coefficients, 0.025s window size, 0.01s step size) using an embedding function  $f^{\text{emb}}$  that contains a 2-layer LSTM with 256 hidden units. Composition function  $g$  is defined as  $g(x_a, x_b) = W_1 x_a + W_1 x_b + W_2(x_a \odot x_b)$ , where  $W_1, W_2$  are learnable weights and  $x_a, x_b$  are speaker embeddings.  $f^{\text{emb}}$  and  $g$  were optimized jointly. During training, 15 audio samples from 5 unique speakers (5 labeled with 1 speaker and 10 with 2 speakers) are used to extract reference speaker embeddings using  $f^{\text{emb}}$ . 20 query speaker embeddings were extracted from the same 5 speakers using  $f^{\text{emb}} \& g$ , with audio or audio pairs  $\{\{1\}, \{2\}, \{3\}, \{4\}, \{5\}, \{1,1\}, \{2,2\}, \{3,3\}, \{4,4\}, \{5,5\}, \{1,2\}, \{1,3\}, \{1,4\}, \{1,5\}, \{2,3\}, \{2,4\}, \{2,5\}, \{3,4\}, \{3,5\}, \{4,5\}\}$ . The distances between reference embeddings and query embeddings are computed and the model is optimized using triplet loss so that the distance between a reference-query pair share the same label is smaller than that of other pairs. After training, the model achieves overall accuracy of 86.9% on a validation set where each episode contains 20 queries as above.

After function  $f^{\text{emb}}$  and  $g$  are trained, we selected hyperparameters of clustering methods based on a separate validation set and then tested on test set. Both the validation set and test set contain 10 groups of data, and all clusters have the same number of samples in each group of data. (For example, in the setting of  $l = 3, n = 120$ , there are 6 clusters with labels  $\{1\}, \{2\}, \{3\}, \{1, 2\}, \{1, 3\}, \{2, 3\}$  and each one has 20 samples.) For all methods, hyperparameters are selected for  $l = 3$  and for  $l = 5$  (both  $n=150$  and  $n=495$ ) separately. For CAP/CAP $\subset$  and AP, there is only one hyperparameter,

$\gamma$ , which we varied over the set  $\{1, 2, \dots, 7\}$ . For AC, there is a distance threshold hyperparameter, which we varied over  $\{1, 2, 3, 4, 4\}$ . These sets of values were chosen in pilot experimentation to give a fair chance to each algorithm; in particular, they were chosen so that the best result, during the validation process, did not fall on the boundary of these sets. During the message-passing process, we damped the values returned by ComputeAlphaStats and ComputeRhoStats using a damping value of  $\lambda = 0.65$ :  $\text{Value} = \text{OldValue} * \lambda + \text{NewValue} * (1 - \lambda)$ . This value for  $\lambda$  was used for CAP, CAP $\subset$ , and AP.

## Appendix F. OmniGlot

OmniGlot contains images of handwritten symbols from a variety of languages. Figure 4 shows 4 groups of examples used in the experiment. Each group contains images with cluster labels  $\{1\}, \{2\}, \{3\}, \{1, 2\}, \{1, 3\}, \{2, 3\}$ .

**Compositional embedding model:** For the image embedding function  $f^{\text{emb}}$  we used ResNet18. Composition function  $g$  is defined the same as for LibriSpeech. The training procedure of  $f^{\text{emb}}$  and  $g$  are the same as for LibriSpeech. After training, the embedding model achieves overall accuracy of 75.0% on validation set.

After function  $f^{\text{emb}}$  and  $g$  are trained, the hyperparameters are selected in the same way, and from the same sets, as in the LibriSpeech experiment. We used damping just like for LibriSpeech.